SOFT ROBOTICS
Volume 6, Number 1, 2019

DOI: 10.1089/soro.2018.0063

SoRo
Soft Robotics

ORIGINAL ARTICLE

Origami-Based Vacuum Pneumatic Artificial Muscles with Large Contraction Ratios

Jin-Gyu Lee and Hugo Rodrigue

Abstract

A novel linear actuator called origami-based vacuum pneumatic artificial muscle (OV-PAM) is proposed in this study that can produce large forces (>400 N) with a contraction ratio >90% of the active length of the actuator. Moreover, some of the designs presented in this article can lift large loads with large contraction ratios at extremely low vacuum pressure ($\approx$10 kPa). This actuator consists of a sealed origami film chamber connecting a polygonal top and bottom plate with evenly spaced transversal reinforcements that prevent the chamber from contracting laterally at certain points of the actuator under vacuum pressure. As vacuum pressure is applied, both a tension force in the walls and a vertical force on the bottom plate of the actuator generate a large contractile force, and the force on the bottom plate can produce a consistent force throughout the entire motion. A quasistatic analytical model was developed that can accurately predict the behavior of the actuator and that can be used for actuator design. OV-PAMs are lightweight, have large contractile forces throughout their entire motion and large contraction ratios. It can also produce large forces at low pressures with large cross-sectional areas. Their versatility could make them well suited for a wide range of applications. They could take us closer to a future where robots can cooperate with humans to shape a better future.

Keywords: vacuum actuator, origami, pneumatic artificial muscle, soft robots

Introduction

Developing machines with which humans can directly and safely interact has been a long-standing challenge of roboticists. Although motor-based robotic arms have been commonplace in factories for decades, it is the natural compliance of artificial muscles that will be useful in bringing robots closer to humans through applications in collaborative robots, service robots, wearable devices, and medical instruments.[1–3] However, one of the main challenges in implementing artificial muscles in real applications is the development of soft actuation technology with the right combination of force, displacement, and speed. This article introduces a new design for an origami-based vacuum pneumatic artificial muscle (OV-PAM) that can realize extremely large deformations (>90% contraction) and large contractile forces through their entire contraction lengths.

A wide range of smart materials capable of producing linear deformations that have been proposed include electroactive polymers, shape memory alloys, shape memory polymers, and twisted-coiled actuators. However, these actuators require either high voltage as in the case of electroactive polymers (>1 kV),[4,5] have limited strains as shape memory alloy wires (<8%),[6] or offer too significant trade-offs between force and displacement.[7–9] Twisted-coiled artificial muscle actuators have good strain and stress but require pre-tension to actuate.[10] Phase change materials and electrically driven hydrogels have been shown to produce large forces and large displacements, but they require external stimuli to begin changing phase and their phase reversal is often slow.[11–13] Combustion-based actuation can nearly instantly produce large motions and forces but is not well suited for controllable kinematics and could present significant dangers for use around humans.[14] Motor and tendon systems have been used to produce linear actuations, but are limited by tendon routing and the use of motors such that they do not suit all applications.[15,16]

Despite these developments in smart material-based artificial muscles, fluid-based actuation remains the actuation method most likely to find significant application in human-scale robots. Pneumatic artificial muscles (PAMs), also called

School of Mechanical Engineering, Sungkyunkwan University, Suwon, South Korea.

McKibben muscles, have large scalable forces and have found significant use in robots of all scales.[17–20] Series PAMs composed of multiple PAMs in series made from a single body have been developed and used in continuum manipulators.[21] However, PAM designs have a limited linear contractile stroke of 36.3% of their length.[22] To solve this issue, inverse PAMs have been developed where the volume decreases and the actuator contracts as the pressure is reduced and are capable of 75% stroke length.[23] Pouch motors made from bonded films for applications requiring lightweight actuators have been developed.[24] Another solution has been to increase the pressure in the bellow to lengthen the actuator by up to 500% of the body's original length.[25] Fluidic elastomer actuators display incredibly life-like motions but operate on a similar principle to McKibben muscles for linear actuation.[26–29] Origami-based elastomeric actuators have shown large and diverse deformations, with fiber-reinforced origami robotic actuators being able to produce contraction ratios up to 50%.[30,31] High-contraction ratio PAM have been developed where a polymeric actuator expands in the lateral direction when pressurized that causes an inextensible diamond-shaped band to contract in the longitudinal direction by up to 64.7%.[32]

Vacuum-actuated muscle-inspired pneumatic structures made from buckling elastomers produce strains up to 45% of their length, but the polymeric structure stores and releases elastic energy diminishing the useful work produced by the actuator and requires thicker vertical beams to obtain the desired deformation.[33,34] A similar actuator was developed where the horizontal compression of the actuator could be translated into a vertical deformation, but the force is limited by the softness of the horizontal beams in the structure for larger loads.[35] Fluid-driven origami-inspired artificial muscles (FOAMs) using a skeleton with a repeated zigzag pattern in a sealed bag made from thin film where the zigzag skeleton compresses as the film shrinks into the gaps of the skeleton's pattern have shown extremely large maximum linear deformations (>90%) and maximum blocked stresses ($\sim$600 kPa).[36] However, the linear force produced by the actuator decreases significantly in the early part of the deformation as the volume decreases rapidly and becomes nearly zero at maximum contraction. For example, a tested actuator produced a maximum linear contraction of 60% with a 1 kg load and of 20% with a 3 kg load. Vacuum-powered soft pneumatic actuators with a foam core have also been used to produce 2 degrees of freedom joints.[37] Alternating negative and positive pressures in a singly body have been used to develop pipe climbing robots that contracts and expands its body.[38]

Most soft linear actuators have either limited strain or have an actuation force that diminishes to zero throughout the motion. This article introduces a new type of OV-PAM, which is a simple actuator that can contract up to 99.7% of its active lengths while producing large forces throughout the entire stroke even at low pressures. An actuator presented in this article was able to lift a weight of 10 kg over a length of 80 mm, equal to 89% of its active length, while weighing only 53.0 g; another was able to lift 40 kg with a contraction of 87%, or 8 kg with a contraction ratio of 85% at only 10 kPa of vacuum pressure. The design of the actuator and its assembly method are presented, followed by a model to predict their performance, and a study of their actuation characteristics. Results show that this type of actuator could be useful for a wide range of applications.

Materials and Methods

Concept and assembly

The actuator consists of a sealed film chamber made from polyvinyl chloride (PVC) film with a thickness of 70 μm connecting a top and a bottom plate with evenly spaced transversal reinforcements that prevent the lateral contraction of the internal bellows of the actuator. There is no direct connection between the reinforcements, unlike FOAMs. Because of this, the cross-sectional area of the bellow remains relatively constant throughout the contraction and it allows OV-PAMs to produce large contractile motions throughout the entire motion (Fig. 1a) (See Supplementary Video S1). To minimize the contracted length of the actuator, the cross-section of the actuator presented in this study is shaped as an equilateral triangle and the film is folded in a modified Yoshimura pattern to allow the film to fold in an even and ordered manner (Fig. 1b) until the actuator is fully contracted (Fig. 1c). The use of this pattern makes the minimum thickness between the reinforcements of twice the thickness of the film at the corners of the top and bottom plates, and four times in the corners of the triangle. The use of any other polygonal shape would produce the same effect, but the use of a circular chamber would result in uneven and unordered folds upon actuation resulting in a smaller and uneven contraction.

The reinforcements and the top and bottom plates are three-dimensionally printed using polylactic acid filament, and the pattern is drawn on the film to visually assist in positioning of the elements within the actuators (Fig. 1d). The film is sealed on one edge using tape to form a tube, and then the reinforcements are positioned in the film and held in place using tape. The top and bottom corners of the film are cut to form flaps that are then folded onto the top and bottom plates and taped onto the plates. Finally, the sections of film between reinforcements are pushed in manually to define the pattern of deformation of the film during actuation. At rest the reinforcements are held in place using the tape and are also strongly held in place during actuation by the force generated by the film on both sides of the reinforcements.

Quasistatic model

The actuator's behavior can be approximated using a quasistatic model where the actuation of the OV-PAM is driven by two forces: a vertical force F_B generated by the vacuum pressure acting on the bottom plate, and a tension force F_T generated by the vacuum pressure on the side walls of the chamber. The contractile force generated by the actuator can be expressed as follows:

$$\sum F = F_B + F_T \tag{1}$$

The equilibrium of output work W_{out} and input work W_{in} can be used to calculate F_T where the work of the fluid in the chamber corresponds to a linear movement dL such that

$$-FdL = PdV \tag{2}$$

The volume of each chamber between two reinforcements can be approximated at low contraction ratios by a triangular prism where three surfaces fold inward with a cylindrical shape (Fig. 2a). The volume of the cylindrical shape as a function of θ

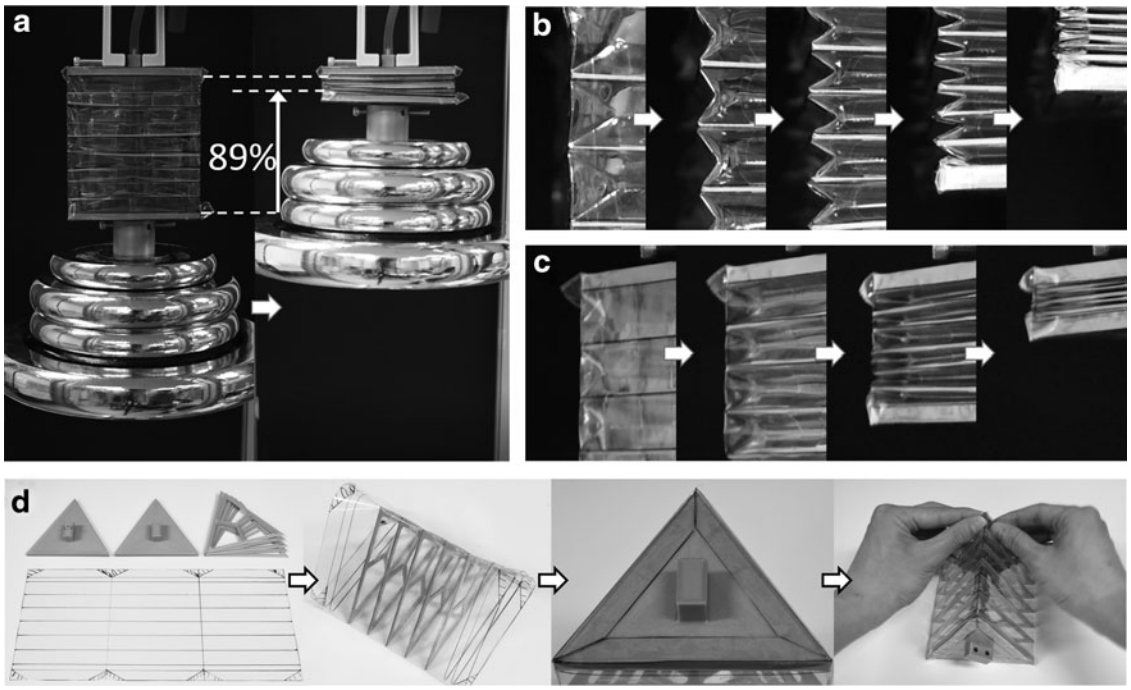

FIG. 1. **(a)** Contraction of the actuator with a load of 10 kg, **(b)** folding of the corners of the actuator, and **(c)** compression of the actuator. **(d)** Manufacturing steps of the actuator.

was derived for previously developed pouch motors,[24] and the volume of the chamber can be derived as follows:

$$V(\theta) = \frac{\sqrt{3}}{4}D^2L - 3A_CD = \frac{\sqrt{3}}{4}D^2L_0\frac{\sin\theta}{\theta} - \frac{3L_0^2D}{4}\left(\frac{\theta - \cos\theta\sin\theta}{\theta^2}\right) \quad (3)$$

where V is the volume of the chamber, D is the width of each triangular sides, L is the length between two reinforcements, A_C is the cross-sectional area of each of the cylindrical sides, L_0 is the initial height of the chamber between two reinforcements and θ is the central angle of the circular segment of the cylindrical sides. The work equilibrium can then be written as follows:

$$F(\theta) = -P\frac{dV}{dL} = -P\frac{\frac{dV}{d\theta}}{\frac{dL}{d\theta}} = -\frac{\sqrt{3}}{4}D^2P - \frac{3}{2}L_0DP\frac{\cos\theta}{\theta} \quad (4)$$

As a negative pressure is applied, a positive force is generated by the film folding inwards of the chamber of the actuator that tends to zero as the angle θ reaches 90° and the contraction ratio reaches $\sim$36.3%. The proposed actuator continues to produce a contractile force past this point because of the vacuum pressure applied on the bottom plate. However, it can be observed that the film starts to stick to the reinforcements, top and bottom plate, and to adjacent films from other chambers starting from approximately this range of deformation. The shape of the film will be approximated as a half cylinder connected horizontally to the edges of the reinforcements such that the diameter of the half cylinder decreases to 0 as the contraction ratio increases to 100% (Fig. 2b). The length of the film is conserved between the reinforcements such that

$$L_0 = 2L_h + L_c \quad (5)$$

where L_h is the length of the horizontal segments of the film and L_c is the length of the film on the cylindrical portion of the

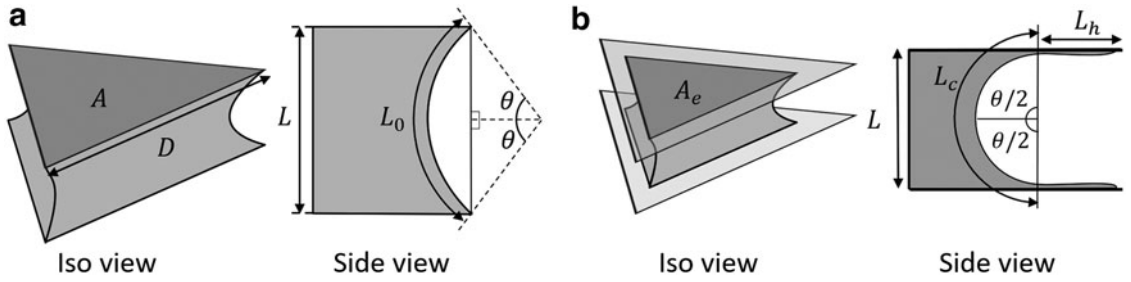

FIG. 2. **(a)** Actuation shape of the actuator in the isometric and side views before reaching a contraction ratio of 36.3%, and **(b)** after 36.3%.

film. As the films begin to stick to the base plate, the effective area A_e decreases and can be calculated based on geometry as given hereunder:

$$A_e = \frac{\sqrt{3}}{4}\left(D - \frac{3L_0 - 1.5L\pi}{\sqrt{3}}\right)^2 \quad (6)$$

If the distance between reinforcements is not too large such that the effective area of the triangle remains positive, the force can then be calculated as:

$$F(L) = -PA_e = -P\frac{\sqrt{3}}{4}\left(D - \frac{3L_0 - 1.5L\pi}{\sqrt{3}}\right)^2 \quad (7)$$

The force is then calculated using Equation (4) at contraction ratios below 36.3% and using Equation (7) at contraction ratios above 36.3%. Quasistatic equilibrium of the actuator is achieved when the force generated by the actuator is equal to the payload.

Experimental method

Vacuum pressure is applied to the actuator using a small vacuum pump (BTC IIS; Parker) and an electropneumatic vacuum regulator (ITV-0090; SMC). The actuator is attached on one end to a load cell (CB1-50kgf; DaCell) and its deformation is measured using a linear encoder (LM10; RLS); the other end of the actuator is used to either attach the applied load or to connect the actuator to a fixed bar to measure the blocking force.

Results

Various properties of the actuator are tested and compared with the model to see whether it can be used as a design tool in future use of this type of actuator. In the first subsection, the basic actuation properties of the actuator with fixed dimensions are tested, then the effect of varying different geometrical dimensions of the actuator, an actuator with flexible top and bottom plates that can reach a contraction ratio of $\sim$100%, and an actuator capable of lifting 40 kg for its entire active length is presented.

Characterization of base actuator

An actuator with representative dimensions was built where the triangular elements have a side length of 90 mm, an active length of 90 mm, and five evenly spaced transversal reinforcements with a thickness of 1 mm each. The actuator weighs 53.0 g. Weights ranging from 1 to 14 kg were attached at the end of the actuator, and the vacuum pump was connected directly to the actuator to measure its maximum contraction ratio depending on load. It is to be noted that the pump used in these experiments has a maximum vacuum pressure of 84.7 kPa, and that loads above 140 N caused the actuator to tear and lose pressure. The actuator is capable of contraction ratios of nearly 90% even with loads nearly 200 times greater than its own weight (Fig. 3a). It can also be seen that there is a slight increase in the contraction ratio of the actuator that may result from either the sidewalls of the actuator straightening under increased loads or from stretching of the film. The contraction ratio of the actuator slightly reduces for loads of 130 N, but that further testing at maximum pressure was limited by actuator failure. This experiment demonstrates the potential of this actuator to produce sustained forces for large stroke lengths.

The blocked force of the actuator is measured by attaching the free end to a fixed element whose position is varied to measure its blocked force throughout the displacement of the actuator for different vacuum pressures (Fig. 3b). The blocked force was measured by fixing the displacement of the actuator and increasing the pressure from 10 kPa up to a maximum of 50 kPa in increments of 5 kPa, but force measurements at each displacement points were stopped when the force reached a value between 110 and 120 N to prevent tearing of the actuator. At small displacements, the actuator can produce extremely large forces, similar to most of the surveyed pneumatic soft linear actuators, but the point of interest of this design is the force produced in the later portion of the contraction, so the measurement at zero displacement was omitted as the force limit is reached at extremely low pressures. In accordance with

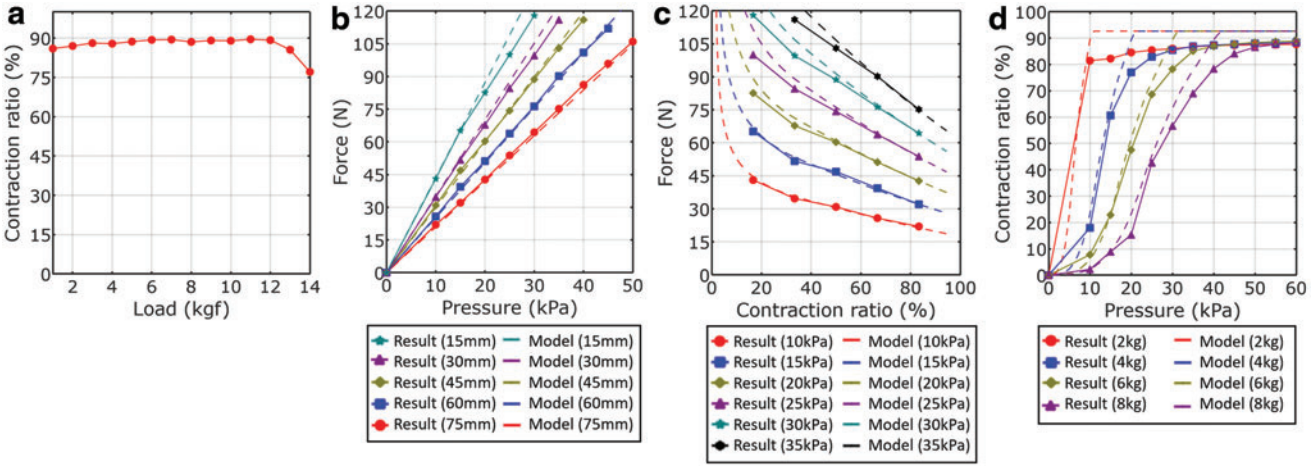

FIG. 3. Results for **(a)** contraction ratio at maximum pump pressure, **(b)** blocked force at different contraction lengths, **(c)** isobaric curves at different pressures, and **(d)** contraction ratio at different pressure points with different payload weights. Color images are available online.

our proposed model, the blocked force increases linearly with an increase in pressure throughout most of the deformation and corresponds very well with the proposed model. Plotting the data as isobaric curves show that for a fixed pressure the force produced by the actuator drops sharply in the initial phase of the displacement but stabilizes as the force generated by the wall tension disappears and the force generated by the vacuum within the bellow continues producing large lifting force (Fig. 3c). The effect of the reduction in effective area is also clearly shown in the later portion of the curves, but there remains a large effective force even at the maximum contraction ratio.

The effect of the payload on the contraction ratio as a function of the vacuum pressure was verified by applying loads ranging from 2 to 8 kg with vacuum pressures ranging from 10 to 60 kPa (Fig. 3d). For small loads, the actuator can lift the load up to its maximum contraction ratio even for very small pressures, and the maximum contraction ratio of the actuator is not affected by the load attached at the tip of the actuator within this range. However, there is a visible transition region for larger applied loads, and this region gets larger as the applied load gets heavier. Although this kind of transition pressure can be seen in other pneumatic actuators, the range of pressure that it spans varies significantly depending on the payload. This is because of OV-PAMs requiring very little force to physically deform, thus requiring low pressures for lighter payloads, whereas other actuators, such as PAMs, need to deform the structure of the actuator to produce a significant deformation. This also means that the deformation of the actuator cannot be predicted without knowing the payload, and that open-loop control of the actuator with unknown payloads will result in highly unpredictable motions.

The model was capable of accurately predicting the effect of pressure and of the payload on the contraction ratio of the actuator throughout most of the motion, and errors compared with the proposed model could be because of differences in the shape of the deformation of side walls during contraction, as a result of manufacturing errors, or because of inaccuracies in pressure or deformation measurements.

Characterization of effect of geometrical dimensions

One interesting property of this actuator is the easy scaling of the length that can be realized by increasing the length of the surrounding film by adding more transversal reinforcements along the length of actuator to keep the distance between each reinforcement the same. This allows to maintain the actuation properties of the actuator in terms of force and contraction by keeping the dimensions of the walls the same between each reinforcement of the actuator. Samples with actuator lengths ranging from 15 to 90 mm were built where the spacing between each of the reinforcement is equal to 15 mm, thus having between zero and five lateral reinforcements. Results were measured with weights ranging from 2 to 8 kg in terms of their normalized contraction ratio (Fig. 4a–d). These results show that the behavior of the actuators is quite similar in terms of force versus contraction ratio regardless of the length of the actuator if the spacing between reinforcements is kept constant throughout the actuator, and that the actuation length and pressure–force behavior of the actuator can be independently selected when designing the actuator. It can also be seen that the contraction ratio of the actuator decreases as the length of the actuator increases, but this is because of the proportion of lateral reinforcements being less for actuators with fewer lateral reinforcements.

The next experiment is to verify the effect of the distance (L_0) between reinforcements on the deformation. Actuators with a fixed length of 90 mm and reinforcement distances of 10, 15, and 30 mm were built, such that they contain 8, 5, and 2 reinforcements, respectively, and were tested for loads ranging from 2 to 8 kg (Fig. 5a–d). Actuators with fewer reinforcements have higher maximum contraction rates as the minimum thickness of the actuator is lower because of the actuated length of the actuator containing fewer reinforcements and fewer folds of film. However, they require more pressure to produce the same displacement with the same payload. It is to be noted that the actuator with a reinforcement spacing of 30 mm failed with a payload of 8 kg. As actuators with fewer reinforcements can produce larger displacements but require a higher pressure to lift the same weight because of a smaller effective area, it is vital to balance both attributes when designing the actuator.

The force of the actuator could be divided into two parts: the tension force generated by the vacuum pressure on the side walls, and the vertical force generated on the bottom plate. Although the former force is proportional to the side length of the actuator, the latter is proportional to the area and thus to the square of the side length. Combined with the minimal force required to deform the structure of the actuator

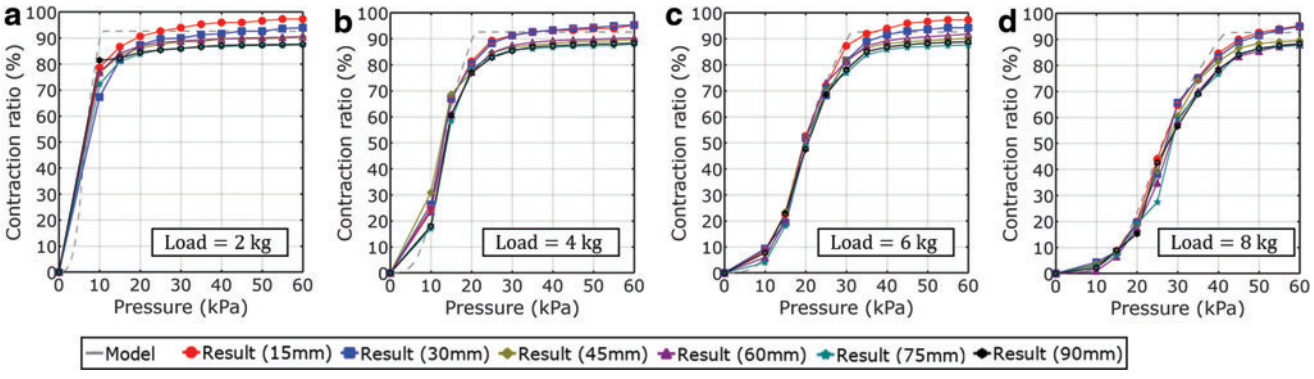

FIG. 4. Contraction ratios for actuator with lengths of 15, 30, 45, 60, 75, and 90 mm and fixed distance between reinforcements (L_0) of 15 mm for loads of **(a)** 2 kg, **(b)** 4 kg, **(c)** 6 kg, and **(d)** 8 kg. Color images are available online.

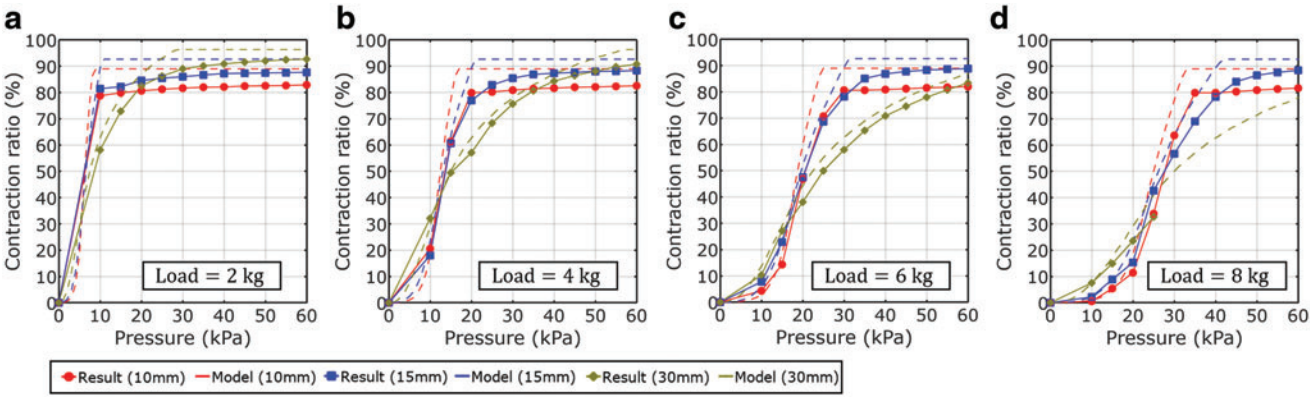

FIG. 5. Contraction ratios for actuators with a fixed length of 90 mm and a distance between reinforcements (L_0) of 10, 15, and 30 mm with loads of **(a)** 2 kg, **(b)** 4 kg, **(c)** 6 kg, and **(d)** 8 kg. Color images are available online.

itself, the area of the actuator is an important property of the actuator that can be changed to significantly alter its actuation property. In addition to being able to lift larger loads for actuators with larger areas, it is also possible to lift similar loads at lower pressures. Low pressure actuation is highly valuable as it allows for safer operation, and for the pneumatic source to operate in a smaller range of pressures where volume flow can be optimized. Contraction tests for actuators with edge lengths of 90, 120, and 150 mm were conducted with loads ranging from 2 to 8 kg for pressures ranging from 0 to 60 kPa of vacuum pressure (Fig. 6a–d). Although all actuators behave similarly with light loads, larger actuators require far less pressure at higher loads to produce large deformations. The largest of the tested actuator is capable of contraction ratios of 85% with a load of 8 kg at only 10 kPa of vacuum pressure. These results show the high potential of this actuator both for lifting very high payloads and for low pressure actuation of high payloads with high contraction ratios.

Flexible top and bottom plates

OV-PAM actuators presented until now had maximum contraction ratios of up to 96% when they did not contain any lateral reinforcements and of ~85–95% depending on the number of lateral reinforcements because of the distance between the top plate and bottom plate being limited by the thickness of the folds and of the lateral reinforcements. However, using flexible top and bottom plates it is possible to further increase the contraction ratio by having the top and bottom plate bend toward each other in the center. It would be possible with this method, in theory, to obtain a contraction ratio of 100% of the active length of the actuator. An actuator with top and bottom plate thicknesses of 1 mm, edge length of 90 mm, an unstretched active length of 90 mm, and five reinforcements spaced 15 mm apart with a thickness of 1 mm each was built to test this concept. This actuator was able to produce a contraction ratio of 99.7% (Fig. 7a) (See Supplementary Video S2). The actuator begins at a stretched active length of 96 mm with

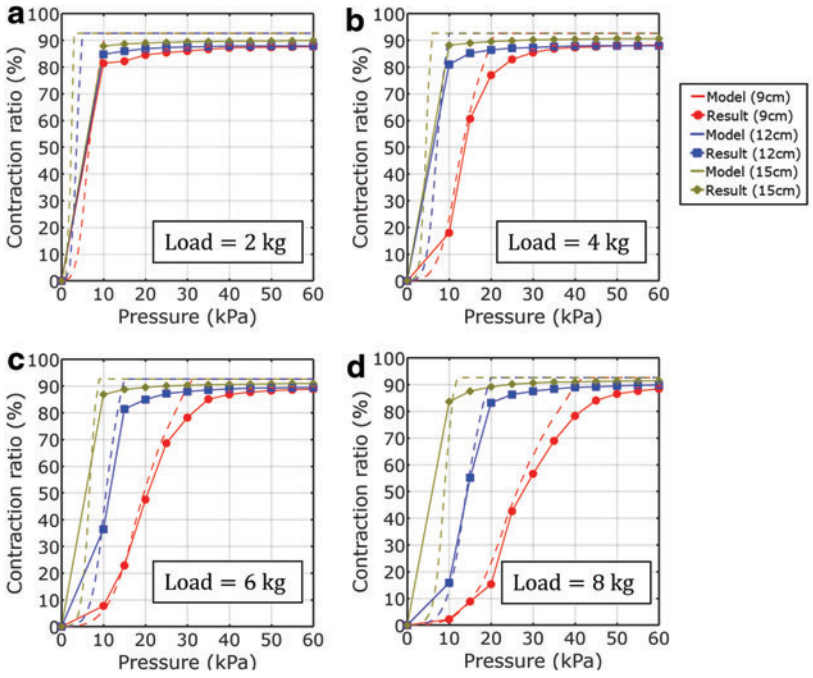

FIG. 6. Contraction ratio for actuators with side lengths of 90, 120, and 150 mm for loads of **(a)** 2 kg, **(b)** 4 kg, **(c)** 6 kg, and **(d)** 8 kg. Color images are available online.

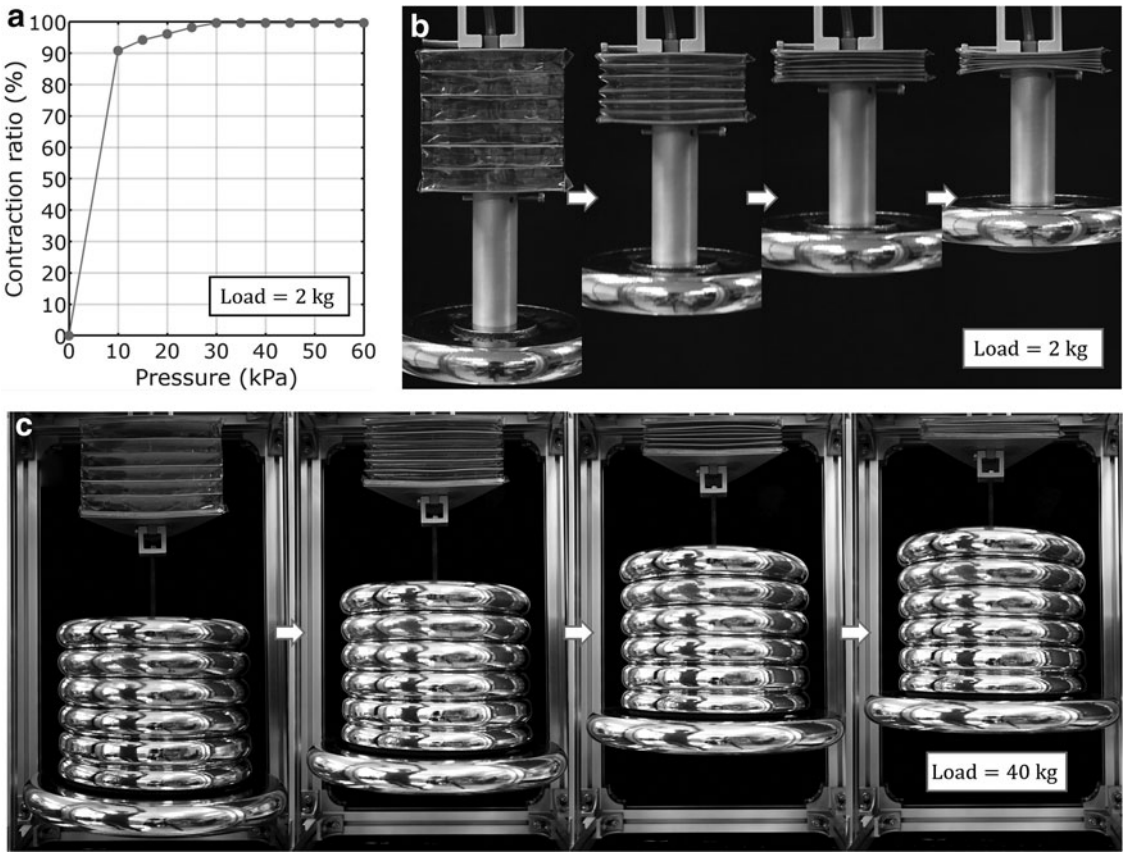

FIG. 7. **(a)** Contraction ratio versus pressure of an actuator with flexible top and bottom plates with a load of 2 kg, and **(b)** its deformation throughout the motion. **(c)** Actuation of an actuator with a side length of 150 mm with a payload of 40 kg.

a payload of 2 kg because of the top and bottom plates bending toward the outside of the actuator, and then maintains this position for most of the contraction. Then, as the actuator approaches its maximum contraction, the top and bottom plates bend in the opposite direction and nearly touch each other to produce a contraction ratio approaching 100% (Fig. 7b). This contraction ratio is the largest achieved among all surveyed soft linear actuators and can be achieved even with a load attached to the actuator.

High force actuation

The actuator with a width of 150 mm was capable of lifting loads of 8 kg at 10 kPa and could, in theory, lift 70 kg at 100 kPa of vacuum pressure. As the force of the actuator can be easily scaled by increasing the cross-sectional area of the actuator, the main limitation for the usable payload is whether the actuator can produce the deformation without breaking. To show that it is possible to lift higher payloads by improving the manufacturing method and materials of the actuator, an actuator with a thicker PVC film with a thickness of 100 μm, rubber bands on the top and bottom plate that function as O-rings, and a second plate at each end used to apply pressure on the flaps to prevent slip was fabricated. This actuator with a weight of 160 g can lift a payload of 40 kg with a contraction ratio of 87% using the same small portable pump as the other actuators (Fig. 7c) (See Supplementary Video S3). This actuator can also lift any loads up to 40 kg for its full contraction length, and it should be possible to lift up to 70 kg if sturdier materials such as aluminum were used for the reinforcements and for the top and bottom plates. Actuators with even larger cross-sections could also lift heavier payloads if all physical aspects of the actuator were reinforced.

Discussions

The OV-PAM actuators presented in this article are capable of contraction ratios up to 100% of their active length and can produce these large contractions while lifting significant payloads. Their actuation curve can be divided into two sections; the early portion of the actuation where the side walls produce a large tension forces that diminishes gradually to zero until a contraction ratio of $\sim$36.3%, and the remainder of the actuation phase where the vacuum force is dominant and nearly constant throughout the entire motion. OV-PAMs have the largest contraction ratio of surveyed PAMs and smart material-based soft actuators and they can lift large payloads for the entirety of their actuation range that allows them to fully actuate for a range of payloads rather than having their contraction ratio depend on the payload, unlike any of the other surveyed soft pneumatic actuators (Fig. 8). Although vacuum-based actuators are limited at 100 kPa of applied pressure, their force is also proportional to the area of the actuator rather than only to its circumference, which allows them to scale significantly by increasing their dimensions.

The OV-PAM would have to be designed with thicker and more robust materials if its intended application required the large forces produced in the early portion of the actuation motion or those produced by larger actuators. The remainder

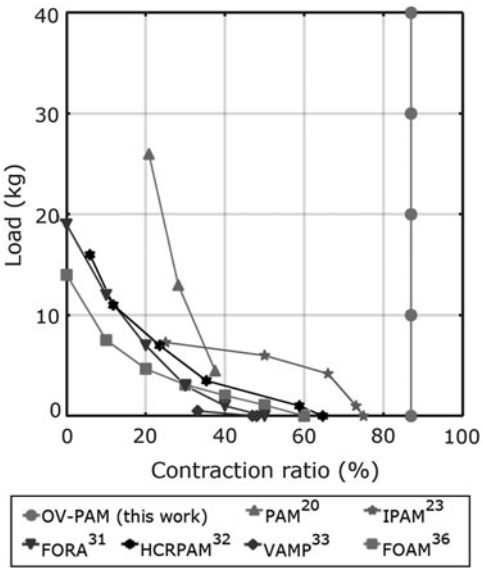

FIG. 8. Comparison of OV-PAM with existing pneumatic linear actuators. OV-PAM, origami-based vacuum pneumatic artificial muscle.

portion of the lift does not require significantly robust materials for repeated actuation for loads in the 1 to 10 kg range, making it possible to use lightweight materials in its construction. Most of the actuators in this article weigh between 40 and 160 g including the top and bottom plates, the intermediate reinforcements, and the parts used to connect the actuator to the pneumatic source and for fixing the actuator mechanically. The specific actuation stress of the actuators presented in this article ranges from 100 to 300 kNm/kg, which is higher than human muscles or traditional pneumatic actuators and comparable with hydraulic actuators but at a much lower weight and with lower implementation requirements.

The vacuum pump used throughout this study is a small and low-cost portable pump weighing 153 g with a voltage of 12 V and a maximum vacuum pressure of 83 kPa that could be easily used in portable applications with batteries. The actuator with a side length of 90 mm and a load of 10 kg requires 2–3 s to actuate, which may not suit applications requiring faster deformations. To solve this problem, larger vacuum pumps could produce faster response speeds that may be required for certain applications, or the parameters of the actuator could be modified to increase the speed with a specific payload. The actuator dimensions could be tailored based on the payload to the properties of the pump to remain within the pressure range with higher flow and efficiency.

The force produced by the vacuum pressure on the bottom plate of OV-PAMs is nearly constant for most of their motion and directly proportional to the vacuum pressure within the chamber. This behavior could make control of the actuator quite difficult, but force applied on the walls of the actuator varies throughout the first portion of the motion, and then the active area of the actuator reduces in the second portion of the motion, allowing the actuator to be controllable. However, as demonstrated in many of the experiments, the amount of pressure required to fully actuate the actuator depends directly on the payload. Thus, open-loop control would be difficult owing to requiring knowledge about the payload to estimate the position of the actuator. Although precise control is not needed in some applications where only a force is required or the actuator should move between two specific positions, a feedback control loop using a strain or force sensor would be required for precise positioning of the actuator. For example, a capacitive sensor could be placed in the connector on the top plate to measure the linear force without significantly impacting the contraction ratio. Another point to consider is that when the payload is much smaller than the maximum payload of the actuator, even a small reduction in actuator pressure allows the actuator to go from the noncontracted position to the fully contracted position. Thus, even applying very little vacuum pressures is enough to cause full actuation if the actuator is designed in consideration of the intended payload.

Conclusion

The OV-PAM actuator presented in this study uses vacuum pressure to deform a chamber made of film with origami folds with rigid lateral reinforcements throughout the length of the actuator. Vacuum pressure causes both the walls of the chambers to apply a vertical tension force and a nearly constant force on the bottom plate of the actuator. This constant force allows the actuator to produce large deformations up to 99.7% of the active length of the actuator. Being made from mainly thin films and plastic, this actuator weighs between 40 and 160 g, but it has been shown to be able to lift weights up to 12 kg for 89% of their active length. Actuators with larger areas were also shown to be capable of lifting 8 kg with a contraction ratio of 85% at pressures as low as 10 kPa or up to 40 kg with a contraction ratio of 87% at higher pressures.

This combination of desirable characteristics not found in previously developed artificial muscles means that OV-PAMs could be useful in a wide range of future robotic applications. They could become one of the leading technologies in soft robotics with applications in wearable robotics, implemented in small and large soft and rigid robots alike, and could take us closer to a future where robots can assist humans in their daily lives and cooperate to shape a better future. Potential applications include soft wearables where their low weight and high specific actuation stress is desirable, as the driving element for surgical tools where length of actuator is a limiting factor, or in low-cost robotic applications for safe industrial or household use through their simple design and force scaling.

Future work will focus on improving the materials and the construction of the actuator to enable testing of its limit in terms of force as current results were limited by the manufacturing method and the properties of the material. In addition, further improvements are required to ensure reliability through repeated actuation, on new designs that minimize the reduction in effective area through the motion, and on the development of control method and of strategies for rapid actuation before its implementation in a wide range of robotic applications.

Acknowledgments

This study was supported by the Technology Innovation Program (or Industrial Strategic Technology Development Program (10080336) funded by the Ministry of Trade, Industry and Energy (MI, Korea), by the National Research Foundation of Korea (NRF) grant funded by the Korea government (Ministry of Science, ICT and Future Planning) (No. 2018R1C1B6003990), and by the convergence technology development program for bionic arm through the

National Research Foundation of Korea (NRF) funded by the Ministry of Science and ICT (No. 2014M3C1B2048175).

Author Disclosure Statement

No competing financial interests exist.

References

1. Kim S, Laschi C, Trimmer B. Soft robotics: a bioinspired evolution in robotics. Trends Biotechnol 2013;31:287–294.
2. Rus D, Tolley MT. Design, fabrication and control of soft robots. Nature 2015;521:467–475.
3. Onal CD, Wood RJ, Rus D. An origami-inspired approach to worm robots. IEEE/ASME Trans Mechatron 2013;18:430–438.
4. Nguyen CT, Phung H, Nguyen TD, *et al.* Multiple-degrees-of-freedom dielectric elastomer actuators for soft printable hexapod robot. Sens Actuators A Phys 2017;267:505–516.
5. Carpi F, Salaris C, Rossi DD. Folded dielectric elastomer actuators. Smart Mater Struct 2007;16:S300–S305.
6. Rodrigue H, Wang W, Han M-W, *et al.* An overview of shape memory alloy-coupled actuators and robots. Soft Robot 2017;4:3–15.
7. Kim S-W, Lee J-G, An S, *et al.* A large-stroke shape memory alloy spring actuator using double-coil configuration. Smart Mater Struct 2015;24:095014.
8. Ruiz S, Mead B, Palmre V, *et al.* A cylindrical ionic polymer-metal composite-based robotic catheter platform: modeling, design and control. Smart Mater Struct 2015;24:015007.
9. Song JJ, Chang HH, Naguib HE. Biocompatible shape memory polymer actuators with high force capabilities. Eur Polym J 2015;67:186–198.
10. Park J, Yoo JW, Seo HW, *et al.* Electrically controllable twisted-coiled artificial muscle actuators using surface-modified polyester fibers. Smart Mater Struct 2017;26:035048.
11. Miriyev A, Stack K, Lipson H. Soft material for soft actuators. Nat Commun 2017;8:596.
12. Liu Z, Calvert P. Multilayer hydrogels as muscle-like actuators. Adv Mater 2000;12:288–291.
13. Bellan LM, Pearsall M, Cropek DM, *et al.* A 3D interconnected microchannel network formed in gelatin by sacrificial shellac microfibers. Adv Mater Res 2012;24:5187–5191.
14. Shepherd RF, Stokes AA, Freake J, *et al.* Using explosions to power a soft robot. Angew Chem Int Ed Engl 2013;52:2892–2896.
15. Asbeck AT, Dyer RJ, Larusson AF, *et al.* Biologically-inspired Soft Exosuit. In: IEEE International Conference on Rehabilitation Robotics (ICORR), Seattle, USA, 2013:1–8.
16. In H, Kang BB, Sin M, *et al.* Exo-Glove: a wearable robot for the hand with a soft tendon routing system. IEEE Robot Autom Mag 2015;22:97–105.
17. Miron G, Plante J-S. Design principles for improved fatigue life of high-strain pneumatic artificial muscles. Soft Robot 2016;3:177–185.
18. Daerden F, Lefeber D. Pneumatic artificial muscles: actuators for robotics and automation. Eur J Mech Environ Eng 2002;47:11–21.
19. Liu X, Rosendo A, Ikemoto S, *et al.* Robotic investigation on effect of stretch reflex and crossed inhibitory response on bipedal hopping. J R Soc Interface 2018;15:20180024.
20. The Shadow Robot Company, UK. Shadow 30 mm air muscle—specification. 2011. Available at: www.shadowrobot.com (accessed November 2, 2018).
21. Greer JD, Morimoto TK, Okamura AM, *et al.* Series pneumatic artificial muscles (sPAMs) and application to a soft continuum robot. In: 2017 IEEE International Conference on Robotics and Automation (ICRA), Singapore, 2017.
22. Tsagarakis N, Caldwell DG. Improved modelling and assessment of pneumatic muscle actuators. In: IEEE International Conference on Robotics and Automation (ICRA), San Francisco, CA, USA, 2000:3641–3646.
23. Hawkes EW, Christensen DL, Okamura AM. Design and implementation of a 300% strain soft artificial muscle. In: 2016 IEEE International Conference on Robotics and Automation (ICRA), Stockholm, Sweden, 2016.
24. Niiyama R, Sun X, Sung C, *et al.* Pouch motors: printable soft actuators integrated with computational design. Soft Robot 2015;2:59–70.
25. Yukisawa T, Ishii Y, Nishikawa S, *et al.* Modeling of extensible pneumatic actuator with bellows (EPAB) for continuum arm. In: 2017 IEEE International Conference on Robotics and Biomimetics, Macau SAR, China, 2017.
26. Shepherd RF, Ilievski F, Choi W, *et al.* Multigait soft robot. Proc Natl Acad Sci U S A 2011;108:20400–20403.
27. Mosadegh B, Polygerinos P, Keplinger C, *et al.* Pneumatic networks for soft robotics that actuate rapidly. Adv Funct Mater 2013;24:2163–2170.
28. Martinez RV, Glavan AC, Keplinger C, *et al.* Soft actuators and robots that are resistant to mechanical damage. Adv Funct Mater 2014;24:3003–3010.
29. Overvelde JT, Kloek T, D'Haen JJ, *et al.* Amplifying the response of soft actuators by harnessing snap-through instabilities. Proc Natl Acad Sci U S A 2015;112:10863–10868.
30. Martinez RV, Fish CR, Chen X, *et al.* Elastomeric origami: programmable paper-elastomer composites as pneumatic actuators. Adv Funct Mater 2012;22:1376–1384.
31. Yi J, Chen X, Song C, *et al.* Fiber-reinforced origamic robotic actuator. Soft Robot 2018;5:81–92.
32. Han K, Kim NH, Shin D. A novel soft pneumatic artificial muscle with high-contraction ratio. Soft Robot 2018. [Epub ahead of print]; DOI: 10.1089/soro.2017.0114.
33. Yang D, Verma MS, So J-H, *et al.* Buckling pneumatic linear actuators inspired by muscle. Adv Mater Technol 2016;1:1600055.
34. Yang D, Mosadegh B, Ainla A, *et al.* Buckling of elastomeric beams enables actuation of soft machines. Adv Mater 2015;27:6323–6327.
35. Yang D, Verma MS, Lossner E, *et al.* Negative-pressure soft linear actuator with a mechanical advantage. Adv Mater Technol 2017;2:1600164.
36. Li S, Vogt DM, Rus D, *et al.* Fluid-driven origami-inspired artificial muscles. Proc Natl Acad Sci U S A 2017;114:13132–13137.
37. Robertson MA, Paik J. New soft robots really suck: vacuum powered systems empower diverse capabilities. Science Robot 2017;2:eaan6357.
38. Verma MS, Ainla A, Yang D, *et al.* A soft tube-climbing robot. Soft Robot 2018;5:133–137.

Address correspondence to:
Hugo Rodrigue
School of Mechanical Engineering
Sungkyunkwan University
2066 Seobu Rd. Jangan–Gu
Suwon 16419
South Korea

E-mail: rodrigue@skku.edu